Funded by the
European Union

Compact

X-band RF electron gun injector design

Daniel González-Iglesias[1], Daniel Esperante[1], Marçá Boronat[1], César Blanch[1], Benito Gimeno[1], Juan Fuster[1], Avni Aksoy[2], Andrea Latina[3], David Alesini[4], Bruno Spataro[4]

[1]Group of Accelerator Physics, Instituto de Física Corpuscular (CSIC-Univ. Valencia), Valencia, Spain

[2]Institute of Accelerator Technologies, University of Ankara, Ankara, Turkey

[3]CERN, Geneva, Switzerland

[4]Istituto Nazionale di Fisica Nucleare - Laboratori Nazionali di Frascati INFN-LNF, Frascati, Italy

Summary

- The main objective is to design a 5.6 cell X-band RF photoinjector fed by a coaxial coupler, the Avni gun prototype has been taken as reference

- Since the entire device (RF gun + coupler) is rotationally symmetric, the RF design was carried out with the 2D software SUPERFISH, which has the advantage of being much faster than full 3D commercial codes such as HFSS or CST

- This design is focused on the optimization of: the resonant frequency, the coupling factor, the maximum values of the RF electric fields in each cavity, the mode separation, and the superficial RF electric field at irises

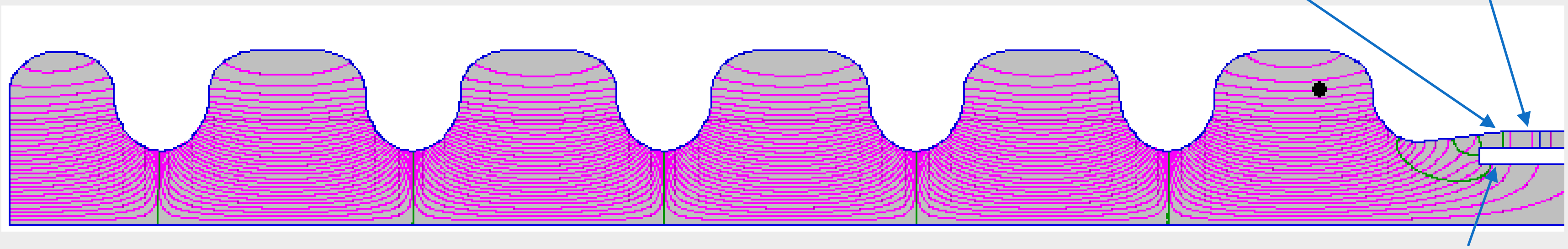

Scheme of a 5.6 cell RF gun with a coaxial coupler

- In the current design it has been taken into account some comments and suggestions made at the XLS First Annual Meeting

RF gun design

- After the optimization, the final dimensions for the RF gun are

$R_{cavity1} = 10.97645\ mm$
$R_{cavity2} = 11.02895\ mm$
$R_{cavity3} = 11.03540\ mm$
$R_{cavity4} = 11.03554\ mm$
$R_{cavity5} = 11.03379\ mm$
$R_{cavity6} = 11.01544\ mm$

$l_{cavity1} = 7.499\ mm$
$l_{cavity2} = 12.498\ mm$
$l_{cavity3} = 12.498\ mm$
$l_{cavity4} = 12.498\ mm$
$l_{cavity5} = 12.498\ mm$
$l_{cavity6} = 12.498\ mm$

$r_{iris} = 4.624 mm$
$r_{corner} = 2.460\ mm$
$a_{iris} = 2.362\ mm$
$b_{iris} = 3.627\ mm$
$r_{iris\ exit} = 5.16815\ mm$
$r_{out} = 5.800\ mm$

$r_{in} = 3.800\ mm$
$a_{iris\ exit} = 2.30821\ mm$
$b_{iris\ exit} = 3.24009\ mm$
$deltar = 1.000\ mm$
$l_{rect} = 4.000\ mm$
$z_{ins} = 2.930\ mm$

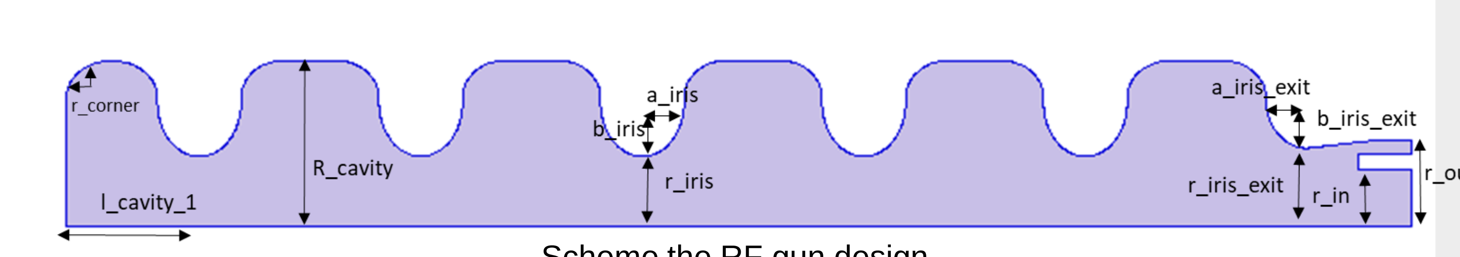

Scheme the RF gun design

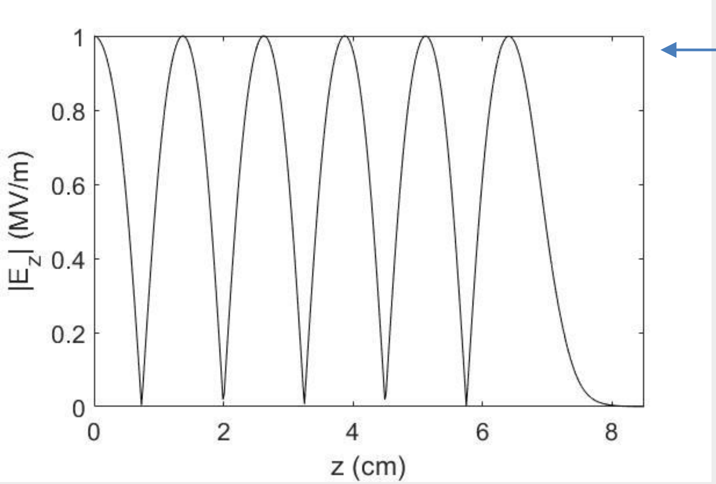

RF electric field maximum flatness is better than 99%

$$f = 11.993996\ GHz$$
$$\beta = 1.005$$

$$\Delta f = 27.1\ MHz$$

$$\max(E_{sup}) = 0.988\ MV/m$$

(for 1 MV/m at cathode axis)

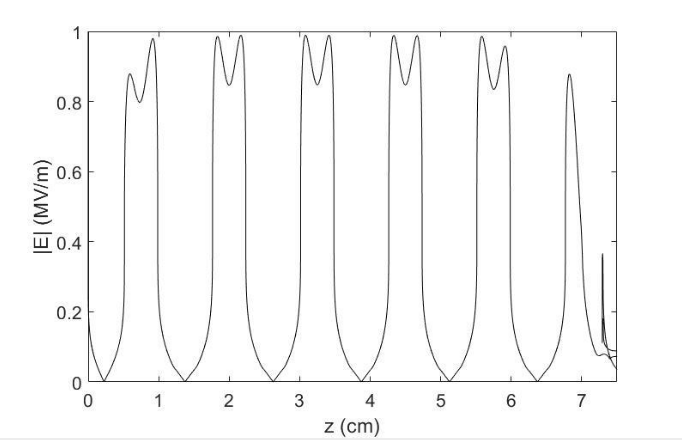

Multipactor analysis in the coaxial coupler

- After the presentation of the first RF gun prototype at the XLS meeting, a concern was expressed about the likely presence of multipactor discharge in coaxial couplers
- Multipactor risk at the coaxial coupler was assessed by means of numerical simulations using our in-house developed code

Numerical simulations were launched at several RF voltage values up to the maximum RF voltage reached at the coaxial coupler

Multipactor zones →

Multipactor window	P (MW)	V(kV)
1	0.035-0.56	0.891-3.565
2	1.20-3.10	5.219-8.388

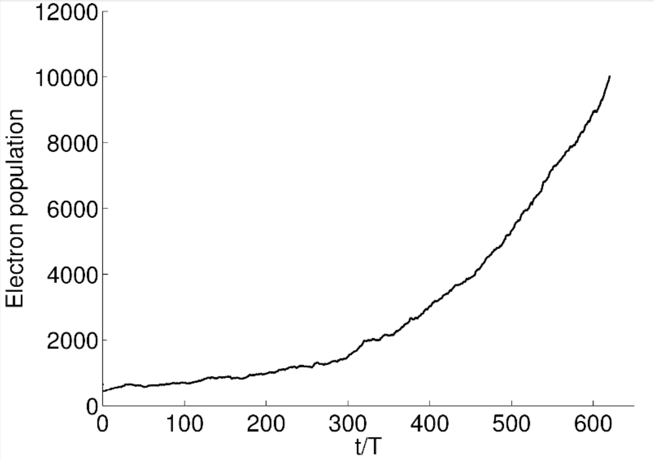

Capture of the output results for the multipactor code

Thus, the coaxial does not suffer multipactor at the steady operating voltage (13.226 kV), however it is likely to appear during the filling of the RF gun cavity

$$V(t) = V_0\left(1 - e^{-\frac{t}{\tau_F}}\right)$$

First window → $\Delta t = 15\,ns,\ \ \Delta t/T = 180$

$$t_F = \frac{2Q_L}{\omega_0} \qquad t_F = 112.5\,ns$$

Second window → $\Delta t = 23\,ns,\ \ \Delta t/T = 276$

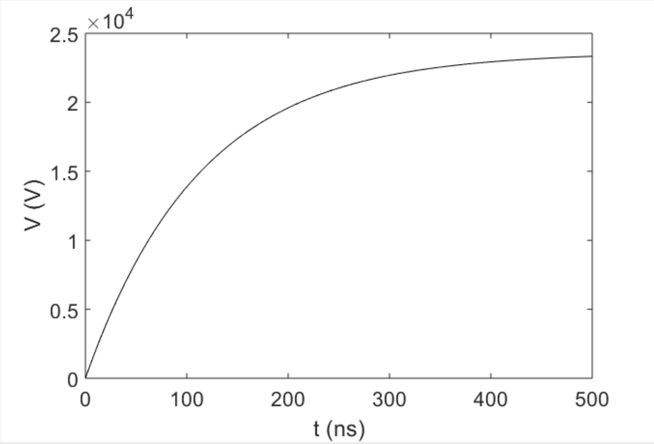

Coaxial voltage amplitude during the cavity filling

Multipactor analysis in the coaxial coupler

- Despite the multipactor risk appearance at the coupler has been evidenced, it is not a crucial problem since it can be suppressed by means of an external magnetic field

- This fact was both theoretically and experimentally demonstrated for a coaxial line[1], thus the following conclusions arise:

  - Multipactor can be suppressed provided that a strong enough magnetic field is applied along the coaxial axis

  - As an approximate rule, the minimum magnetic field to mitigate the discharge is given by

$$f_c \approx f \qquad f_c = \frac{1}{2\pi}\frac{e}{m}B_{dc}$$

f is the RF frequency
B_{dc} is the external magnetic field
m is the electron mass

f_c is the cyclotron frequency
$-e$ is the electron charge

In our case, the above condition gives $B_{dc} = 428.5\ mT$

✓ Numerical simulations support that no multipactor discharge is expected with such external magnetic field

✓ In fact, it is found that a $B_{dc} = 360\ mT$ is enough to suppress the discharge, according to the numerical simulations

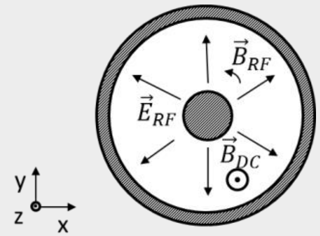

coaxial line transverse cross section

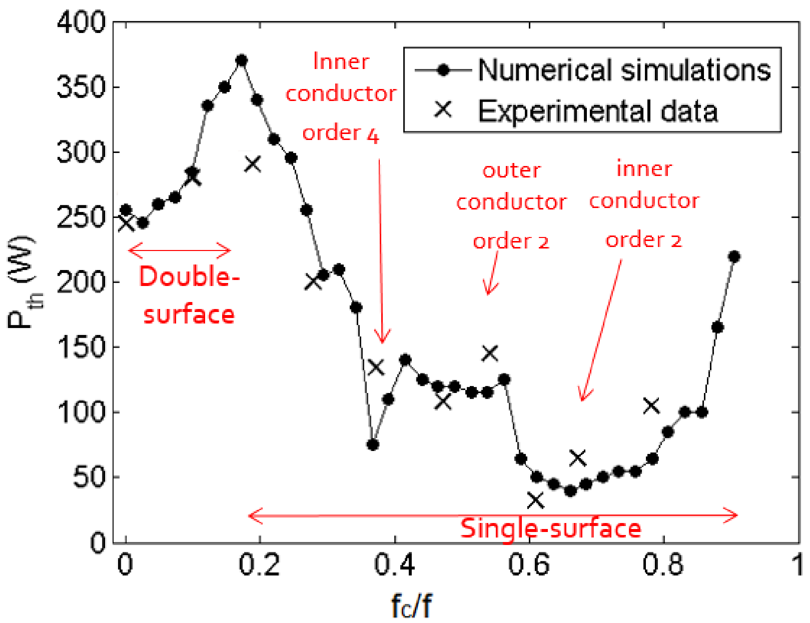

Multipactor RF power threshold as a function of the ratio between the cyclotron frequency and the RF frequency. For a coaxial line at f = 1.145 GHz

[1]D. González-Iglesias et al., "Multipactor Mitigation in Coaxial Lines by Means of Permanent Magnets", IEEE Transactions on Electron Devices, vol. 61, no. 12, pp. 4224-4231, Dec. 2014.

RF breakdown

- The risk of RF breakdown in the component is assessed by means the breakdown rate (BDR), which is obtained by computing the modified Poynting vector[1]

$$BDR \equiv \frac{number\ of\ breadowns}{pulse \cdot 1m\ structure\ length}$$

Complex Poynting vector $\vec{S} = \frac{1}{2}\vec{E} \times \vec{H}^*$

Modified Poynting vector $S_c = \left|Re\{\vec{S}\}\right| + g_c\left|Im\{\vec{S}\}\right|$

$0.15 \leq g_c \leq 0.2$ typically $g_c = {}^1/_6$

On the right it is depicted the S_c value at the RF gun surfaces (using a value of g_c=1/6) for a cathode electric field of 200 MV/m, which is selected as the maximum electric field operating value

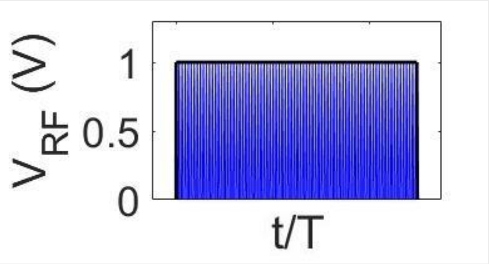

The BDR follows the next empirical law:

$$\frac{S_c^{15} t_p^5}{BDR} = C$$

t_p is the pulse length
C is a constant

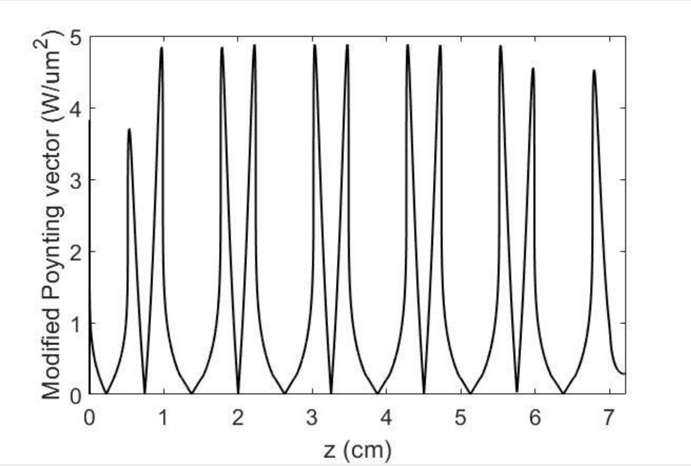

Modified Poynting vector at the RF gun surfaces as a function of the axial position, for cathode field of 200 MV/m

According to ref. (1), a value of S_c = 5 W/μm^2 for a pulse length of 200 ns gives a breakdown rate of BDR = 10^{-6} bpp/m. Using this data, the constant can be evaluated C = 9.765625×10^{27} $W^{15}\cdot ns^5\cdot m\cdot \mu m^{-7.5} bpp^{-1}$

$$BDR = \frac{S_c^{15} t_p^5}{C} \quad \text{(eq. 1)}$$

Maximum modified Poynting vector → $\max(S_c) = 4.88\ W/\mu m^2$

Mean value of modified Poynting vector → $\text{mean}(S_c) = 2.00\ W/\mu m^2$

[1]A. Grudiev et al., "New local field quantity describing the high gradient limit of accelerating structures", Physical Review Special Topics –Accelerators and Beams, 12, 102001 (2009).

RF breakdown

- In eq. 1 is assumed (see ref. 1 of previous slide) that the amplitude of the RF electromagnetic field is constant over the entire RF pulse, whilst in the RF gun case there is a transitory behavior during the filling and emptying of the structure

$$E = E_0 \sin(\omega t) \qquad H_0 = \frac{E_0}{Z} \qquad \vec{S} = \frac{1}{2}\vec{E} \times \vec{H}^* \qquad S \propto E_0^2$$

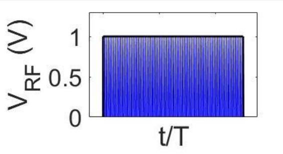

In ref. 1 ⟶ $S_c(t) = S_{c,0}, \quad 0 \le t \le t_p$ ⟶ $BDR = \frac{S_{c,0}^{15} t_p^5}{C}$ (eq. 1)

For the RF gun ⟶

$$S_c(t) = \begin{cases} S_{c,0}\left(1 - e^{-t/t_F}\right)^2, & 0 \le t \le T_{on} \\ S_{c,0}\left(1 - e^{-T_{on}/t_F}\right)^2 e^{-\frac{2(t-T_{on})}{t_F}}, & t \ge T_{on} \end{cases}$$

T_{on} is the time that the RF generator is on
ω is the angular RF frequency
t_F is the filling time of the cavity

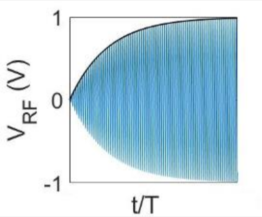

- For the RF gun case, the BDR can be calculated by splitting the RF pulse as the sum of many short pulses, each of them with its corresponding BDR given for the uniform S_c amplitude case of eq. 1:

$$BDR_{pulse} = \sum_{k=1}^{n} BDR(k) = \frac{1}{C}\sum_{k=1}^{n} S_c^{15}(t_k) t_p^5 = \frac{1}{C}\sum_{k=1}^{n} S_c^{15}(t_k)\left(\frac{T_p}{n}\right)^5$$

$$BDR_{pulse} = \frac{1}{C}\lim_{n\to\infty}\sum_{k=1}^{n} S_c^{15}(t_k)\left(\frac{T_p}{n}\right)^5 = \frac{1}{C}\int_0^{T_p} S_c^{15}(t)\, d(t^5)$$

$$\boxed{BDR_{pulse} = \frac{5}{C}\int_0^{T_p} S_c^{15}(t)\, t^4\, dt}$$

$$T_p = n t_p \qquad t_k = k t_p$$

T_p is the pulse length

$$\lim_{n\to\infty}\sum_{k=1}^{n} f(x_k)\Delta x_k = \int_a^b f(x)\, dx$$

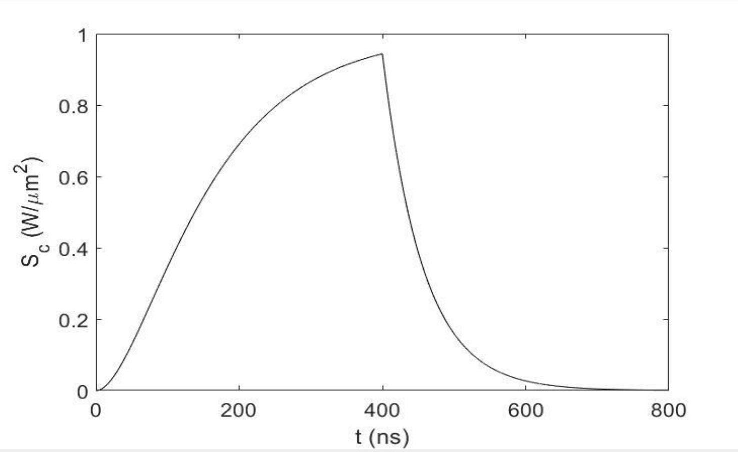

Maximum amplitude of the modified Poynting vector as a function of time

RF breakdown

- Taking into account that for the RF gun, $\max(S_c) = S_{c,0} = 4.88\ W/\mu m^2$, the BDR can be obtained as a function of the pulse length:

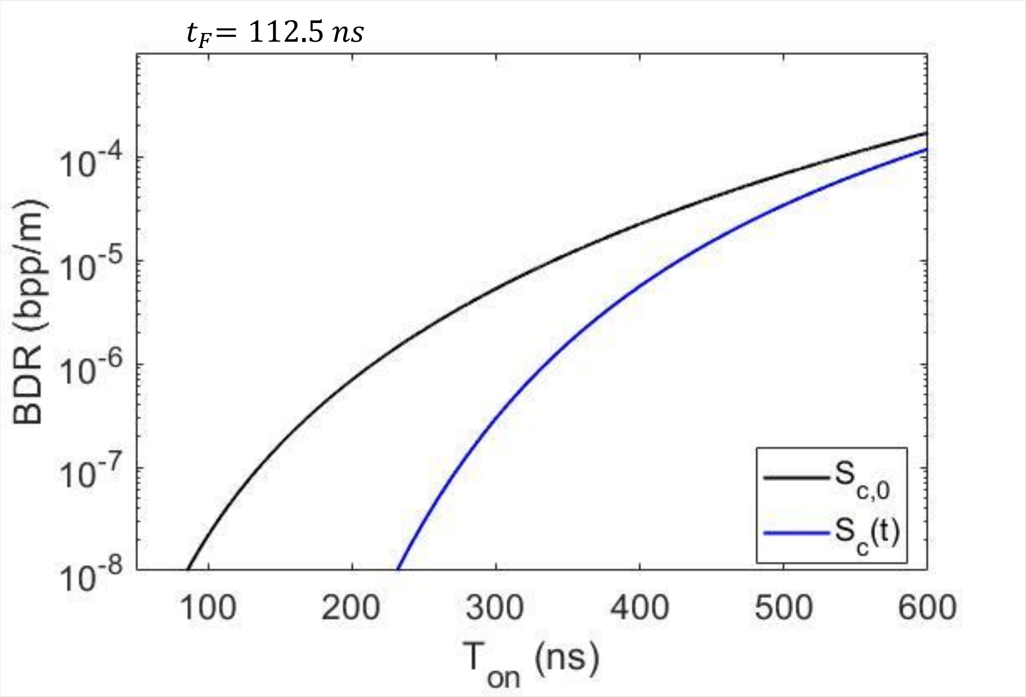

BDR as a function of the time that the generator is on, for the RF gun operating with 200 MV/m at cathode

- In the graph it is depicted the BDR obtained both using the approximation of time-constant RF electromagnetic field ($S_{c,0}$) and computing the integral assuming the time-variation of S_c

$$BDR = \frac{S_{c,0}^{15} t_p^5}{C}$$

$$BDR_{pulse} = \frac{5}{C}\int_0^{T_p} S_c^{15}(t)\, t^4 dt$$

- As it is expected, when $T_p >> t_F$, the BDR calculated by means of integration of S_c tends to the approximated calculation of constant $S_{c,0}$

Funded by the European Union

Compact

RF pulse heating

- RF magnetic field on metallic device surfaces induces electric currents that increases the wall temperature due to Joule effect, this phenomenon is known as RF pulse heating

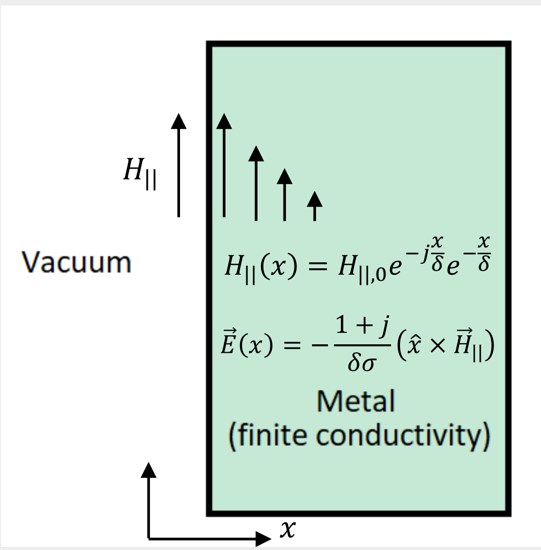

$$P = \frac{1}{2}\int \vec{J}\cdot\vec{E}^{*}dV \qquad P = \frac{1}{2}R_s A\left|H_{||,0}\right|^2 \qquad \frac{P(x)}{A} = \frac{R_s}{2}\left|H_{||,0}\right|^2\frac{2}{\delta}e^{-2x/\delta}$$

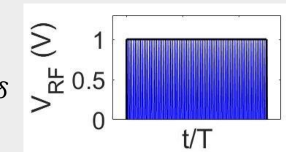

$$\vec{J} = \sigma\vec{E}$$

Heat transfer equation $$\frac{\partial T}{\partial t} = \frac{k}{\rho C_\epsilon}\nabla^2 T + f(\vec{r},t) \qquad R_s = \frac{1}{\delta\sigma} \qquad \delta = \sqrt{\frac{2}{\sigma\mu_0\omega}}$$

An approximate formula describing the temperature rise for a semi-infinite body (1D model) is given in (1):

Temperature rise (approximation) $$\Delta T = \frac{\left|H_{||}\right|^2\sqrt{t_p}}{\sigma\delta\sqrt{\pi\rho C_\epsilon k}}$$

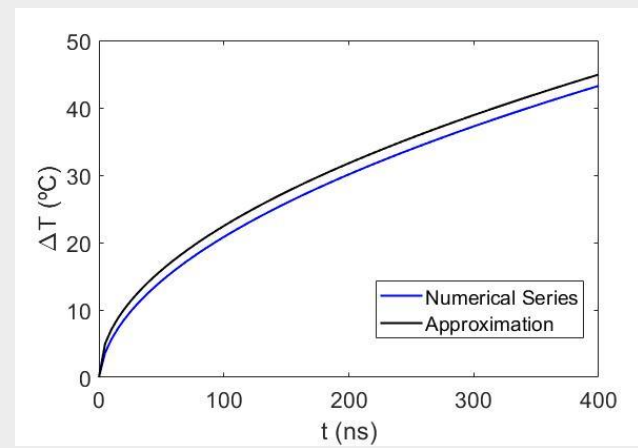

Temperature increase as a function of time

Temperature rise obtained from analytically solving the heat transfer equation

$$\Delta T(x,t) = \frac{\alpha}{L}\left(1-e^{-\frac{2L}{\delta}}\right)t + \sum_{n=1}^{\infty}\left(\frac{L}{\pi n a}\right)^2\frac{8\alpha L}{4L^2+(\pi\delta n)^2}\left(1-e^{-\frac{2L}{\delta}}(-1)^n\right)\left(1-e^{-\left(\frac{\pi n a}{L}\right)^2 t}\right)\cos\left(\frac{\pi n x}{L}\right)$$

$H_{||}$ is the magnetic field parallel to the surface
ρ is the density
ω is the angular frequency
T is the temperature

t_p is the RF pulse length
C_ϵ is the specific heat
μ_0 is the magnetic permeability of vacuum
$f(\vec{r},t)$ are the heat sources

σ is the electric conductivity
k is the thermal conductivity
A is the area
L is the wall length

$$a = \sqrt{\frac{k}{\rho C_\epsilon}}$$

$$\alpha = \frac{1}{2}\frac{R_s}{\rho C_\epsilon}\left|H_{||}\right|^2$$

[1]D. P. Pritzkau, "RF Pulsed Heating", SLAC-Report-577 , Ph.D. Dissertation, Stanford University, 2001.

RF pulse heating

- The previous temperature rise approximation, as well as the exact solution based on the series, are assuming an RF electromagnetic field of constant amplitude in time

- However, this is not true in the RF gun due to the transient during the filling and emptying of the device. This effect must be considered when resolving the heat transfer equation:

$$f(x,t) = \frac{P(x,t)}{A} = \frac{R_s}{2}\left|H_{||,0}(t)\right|^2 \frac{2}{\delta} e^{-2x/\delta} \qquad f(x,t) = g(x)h(t)$$

$$H_{||,0}(t) = \begin{cases} H_{||,0}\left(1 - e^{-t/t_F}\right), & 0 \le t \le t_{on} \\ H_{||,0}\left(1 - e^{-T_p/t_F}\right) e^{-\frac{(t-T_p)}{t_F}}, & t \ge t_{on} \end{cases}$$

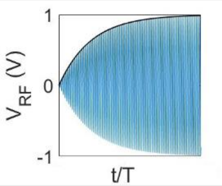

$$\frac{\partial T}{\partial t} = \frac{k}{\rho C_\epsilon}\nabla^2 T + f(\vec{r},t)$$

Heat transfer equation

$$\Delta T(x,t) = \begin{cases} u_0(t) + \sum_{n=1}^{\infty} u_n(t)\cos\left(\frac{\pi n x}{L}\right), & 0 \le t \le t_{on} \\ u_0(t_{on}) + v_0(t) + \sum_{n=1}^{\infty}\left(v_n(t) + u_0(t_{on}) e^{-\left(\frac{\pi a n}{L}\right)^2 t}\right)\cos\left(\frac{\pi n x}{L}\right), & t \ge t_{on} \end{cases}$$

$$g_n = \frac{2}{L}\int_0^L g(\xi)\cos\left(\frac{\pi n \xi}{L}\right) d\xi$$

$$u_0(t) = \frac{g_0}{2}\left[t + t_F\left(2e^{-\frac{t}{t_F}} - \frac{1}{2}e^{-\frac{2t}{t_F}} - \frac{3}{2}\right)\right] \qquad v_0(t) = \frac{g_0 t_F}{4}\left(1 - e^{-\frac{t_{on}}{t_F}}\right)^2\left(1 - e^{-\frac{2t}{t_F}}\right)$$

$$u_n(t) = \frac{g_n\left(1 - e^{-\frac{t_{on}}{t_F}}\right)^2}{\left(\frac{\pi a n}{L}\right)^2}\left[e^{-\frac{2t}{t_F}} - e^{-\left(\frac{\pi a n}{L}\right)^2 t}\right]$$

$$v_n(t) = \frac{g_n}{\left(\frac{\pi a n}{L}\right)^2 - \frac{2}{t_F}}\left(1 - e^{-\left(\frac{\pi a n}{L}\right)^2 t}\right) + \frac{g_n}{\left(\frac{\pi a n}{L}\right)^2 - \frac{2}{t_F}}\left(e^{-\frac{2t}{t_F}} - e^{-\left(\frac{\pi a n}{L}\right)^2 t}\right) + \frac{2 g_n}{\left(\frac{\pi a n}{L}\right)^2 - \frac{1}{t_F}}\left(e^{-\left(\frac{\pi a n}{L}\right)^2 t} - e^{-\frac{t}{t_F}}\right)$$

RF pulse heating

➢ Now, it can be estimated the temperature rise in the photoinjector surfaces for an RF pulse with 200 MV/m at cathode at the stationary state

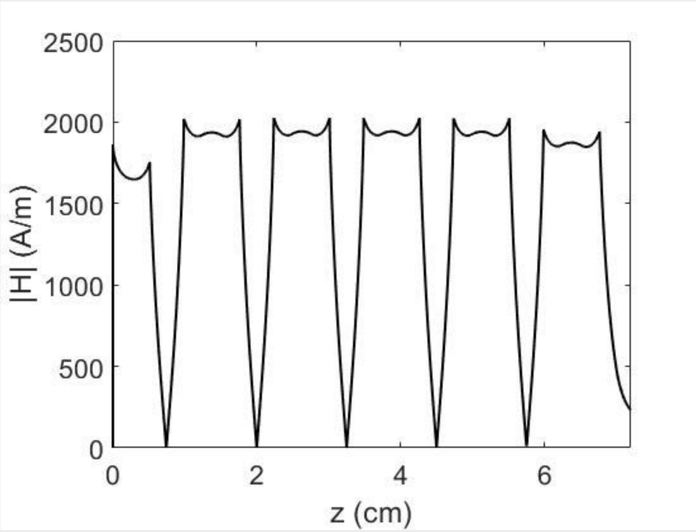

Magnetic field at the gun surfaces as a function of the axial position for 1 MV/m at cathode

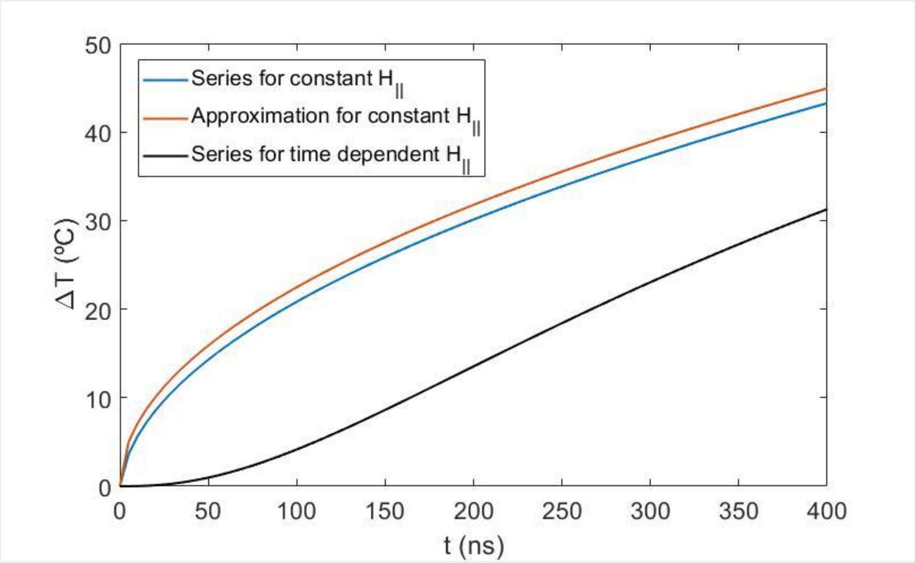

Maximum temperature increase in the RF gun as a function of time

Maximum temperature rise
(for a pulse length of t_p= 400 ns) → $\max(\Delta T) = 31^{o}C$

- This value is below 50ºC, which is the maximum temperature rise suggested by Avni
- Other authors suggest a 60ºC maximum increase[1]

Temperature rise along the RF gun surfaces →

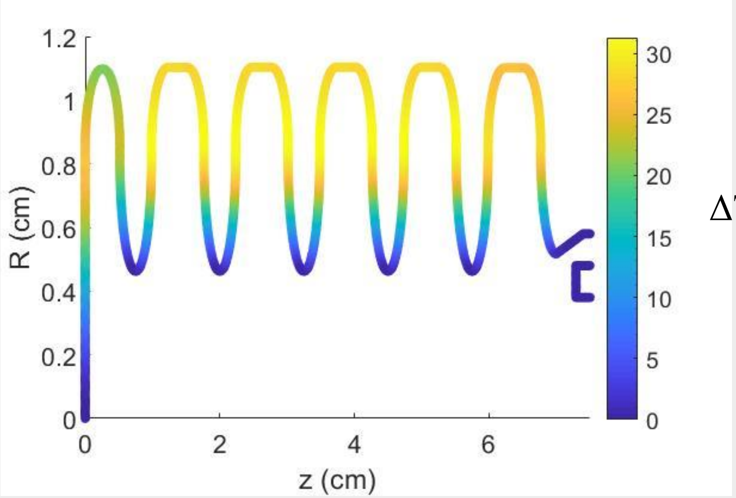

[1]M. Behtouei, "Design and Measurements of the High Gradient Accelerating Structures" PhD Thesis, Università di Roma "La Sapienza", 2018

Study of the effect of neighbour cavity modes

- Despite the RF gun has been designed for operation with the π-mode, other neighbour modes present in the cavity might be excited during the transient regime

- To calculate the excitation of these neighbor modes, it is useful to use a equivalent circuital model to describe the mode excitation in the system composed by the RF generator, the coupler and the RF gun cavity[1,2]

$$\frac{\omega_m}{Q_0}\sqrt{\frac{\beta R}{Z_0}}V_{rf}(t) = \frac{dV_{cav}}{dt} + \frac{\omega_m}{Q_L}V_{cav} + \omega_m^2\int V_{cav}dt$$

$$V_{cav}(t) = V_{cav,0}\left[\sin(\omega t + \varphi_1) - \frac{e^{-\frac{\omega_m}{2Q_L}t}}{\sqrt{1-\frac{1}{4Q_L^2}}}\sin\left(\omega_m\sqrt{1-\frac{1}{4Q_L^2}}\,t + \varphi_2\right)\right]$$

$$V_{cav,0} = V_{rf,0}\frac{\omega_m\omega}{Q_0}\sqrt{\frac{\beta R}{Z_0}}\frac{1}{\sqrt{\left(\frac{\omega\omega_m}{Q_L}\right)^2 + (\omega_m^2-\omega^2)^2}}$$

For $t >> \frac{\omega_m}{2Q_L}$ → $V_{cav}(t) \simeq V_{cav,0}[\sin(\omega t + \varphi_1)]$

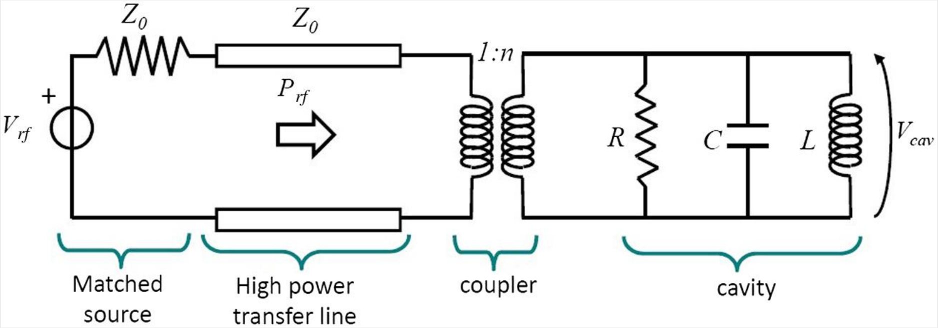

Equivalent circuit describing the RF generator, coupler and gun cavity (extracted from ref. 1)

$$\tan\varphi_1 = Q_L\frac{\omega_m^2-\omega^2}{\omega\omega_m}$$

$$\tan\varphi_2 = \sqrt{4Q_L^2-1}\,\frac{\omega_m^2-\omega^2}{\omega_m^2+\omega^2}$$

β is the coupling factor
ω is the RF generator angular frequency
ω_m is the cavity mode angular frequency
R is the circuit resistance
Q_L is the loaded cavity quality factor
Q_0 is the unloaded cavity quality factor
Z_0 is the high power transfer line impedance
V_{rf} is the RF generator voltage
V_{cav} is the RF voltage in the gun cavity

[1] D. Alesini et al., "Design, realization, and high power test of high gradient, high repetition rate brazing-free S-band photogun", Physical Review Accelerators and Beams. 21, 112001 (2018)
[2] Thomas P. Wangler , "RF Linear Accelerators", Second Edition, 2008 WILEY-VCH Verlag GmbH & Co. KGaA

Study of the effect of neighbour cavity modes

- Thus, the axial RF electric field of the mode cavity m is given by

$$E_{z,m}(z,t) = E_{0,cath,m}(t)\ g_m(z)$$

and the total RF axial electric field in the RF gun due to the superposition of N cavity modes is obtained by means of the linear superposition of them:

$$E_z(z,t) = \sum_{i=1}^{N} E_{z,m}(z,t) = \sum_{i=1}^{N} E_{0,cath,m}(t)\ g_m(z)$$

- For the RF gun, consisting of six cells, there will be five neighbor modes near the operating π-mode that could be excited, even if the RF generator excitation frequency perfectly matches the π-mode frequency

mode	f_m (GHz)	$Q_{L,m}$	β_m	α_m ($Vm^{-1}W^{-0.5}$)
π	11.993996	4238.51	1.00477	42207.155
1	11.9669	2927.36	1.816202	60021.928
2	11.896	3411.46	1.405519	63107.831
3	11.809	4447.77	0.8362	66482.625
4	11.730	6115.44	0.3414	35850
5	11.681	7924.16	0.0722	48378.9

$$E_{0,cath,m} \propto \frac{\omega_m \omega}{\sqrt{\left(\frac{\omega\omega_m}{Q_L}\right)^2 + (\omega_m^2 - \omega^2)^2}}$$

- The amplitude of the excited modes decay as the mode resonant frequency moves away from the RF generator excitation frequency

Study of the effect of neighbour cavity modes

- Since SUPERFISH provides $g_m(z)$ for each cavity mode, the total RF electric field (due to the superimposition of modes) along the gun axis can also be obtained:

$$E_z(z,t) = \sum_{i=1}^{N} E_{0,cath,m}(t)\, g_m(z)$$

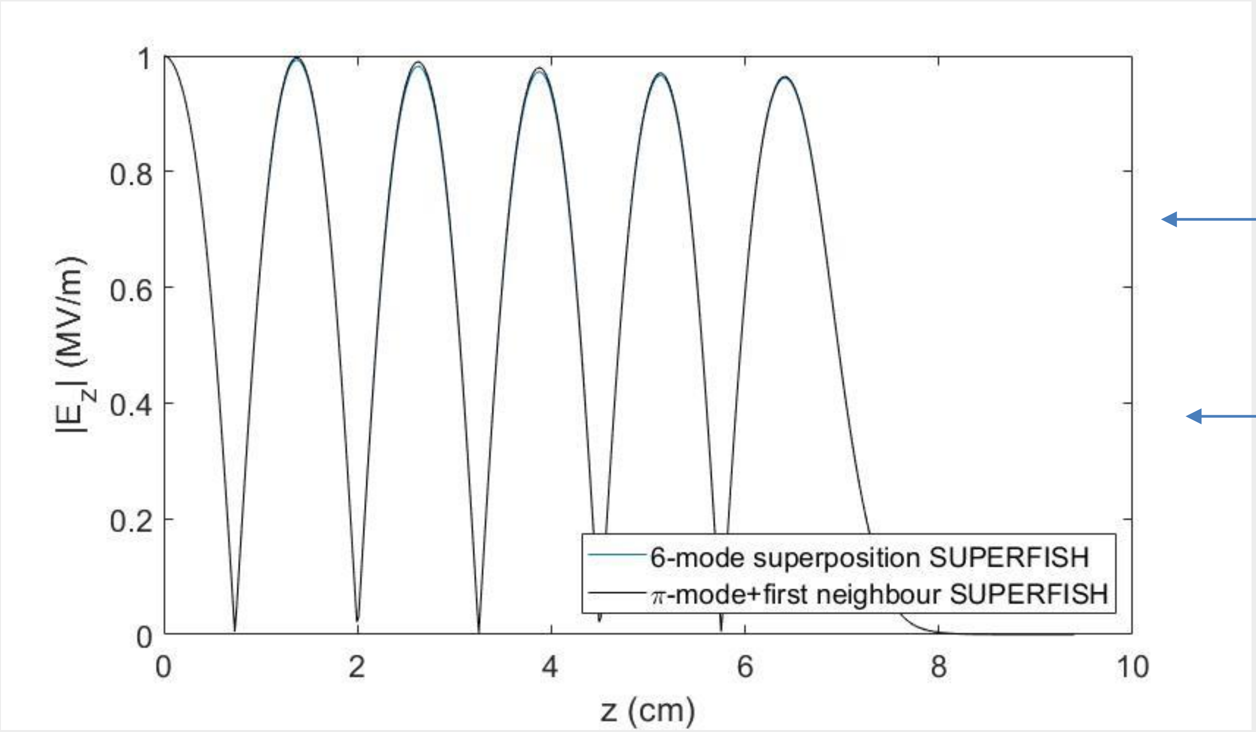

RF electric field along the gun axis at the stationary state (after the transient). Comparison between the case considering the 6 cavity modes vs considering only the π-mode and the nearest neighbor mode.

- It is observed no difference between the two cases, therefore it is enough to consider the π-mode and the nearest neighbor mode
- Slight decrease in the maximum RF electric field amplitude at last cavities due to the neighbor mode presence

For $t >> \frac{\omega_m}{2Q_L}$ → $$E_z(z,t) = \sum_{i=1}^{N} E_{0,cath,m} \sin(\omega t + \varphi_m)\, g_m(z)$$

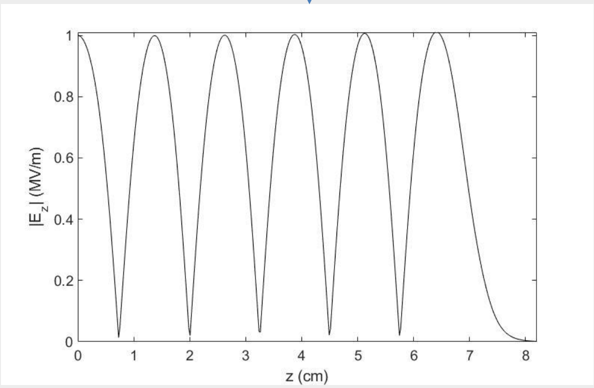

RF electric field along the gun only for π-mode

Study of the effect of neighbour cavity modes

- The consideration of the neighbor mode has revealed a slight distortion of the RF electric field profile (specially at the last gun cavities) from the original design goal, i.e., all cavities with the same maximum RF electric field amplitude

- Thus, a re-design of the RF gun taking the nearest neighbor mode has to be performed in order to correct such RF electric field distortion. After this, the following RF gun design arises:

$R_{cavity1} = 10.97642\ mm$
$R_{cavity2} = 11.02921\ mm$
$R_{cavity3} = 11.03551\ mm$
$R_{cavity4} = 11.03548\ mm$
$R_{cavity5} = 11.03354\ mm$
$R_{cavity6} = 11.01467\ mm$

$l_{cavity1} = 7.499\ mm$
$l_{cavity2} = 12.498\ mm$
$l_{cavity3} = 12.498\ mm$
$l_{cavity4} = 12.498\ mm$
$l_{cavity5} = 12.498\ mm$
$l_{cavity6} = 12.498\ mm$

$r_{iris} = 4.624 mm$
$r_{corner} = 2.460\ mm$
$a_{iris} = 2.362\ mm$
$b_{iris} = 3.627\ mm$
$r_{iris\ exit} = 5.16168\ mm$
$r_{out} = 5.800\ mm$

$r_{in} = 3.800\ mm$
$a_{iris\ exit} = 2.31036\ mm$
$b_{iris\ exit} = 3.24023\ mm$
$deltar = 1.000\ mm$
$l_{rect} = 4.000\ mm$
$z_{ins} = 2.930\ mm$

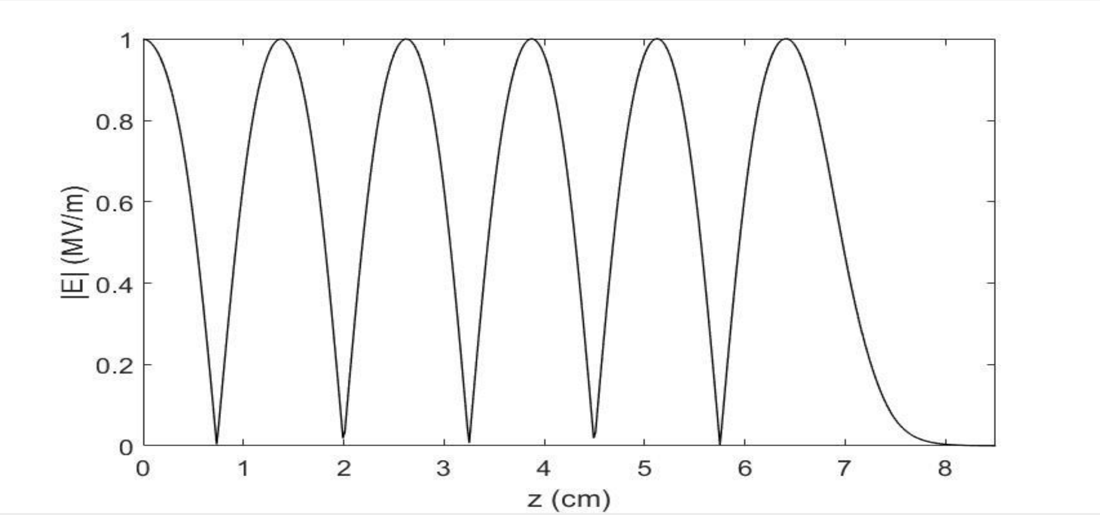

$f = 11.9940380 GHz$
$\beta = 1.027$

$\Delta f = 27.1\ MHz$

$\max(E_{sup}) = 0.988\ MV/m$

(for 1 MV/m at cathode axis)

RF electric field maximum flatness is better than 99%

Summary

- The RF electric and magnetic fields patterns along the device surfaces are compared with regard to the previous RF gun design (which was analyzed considering only the presence of the π-mode)

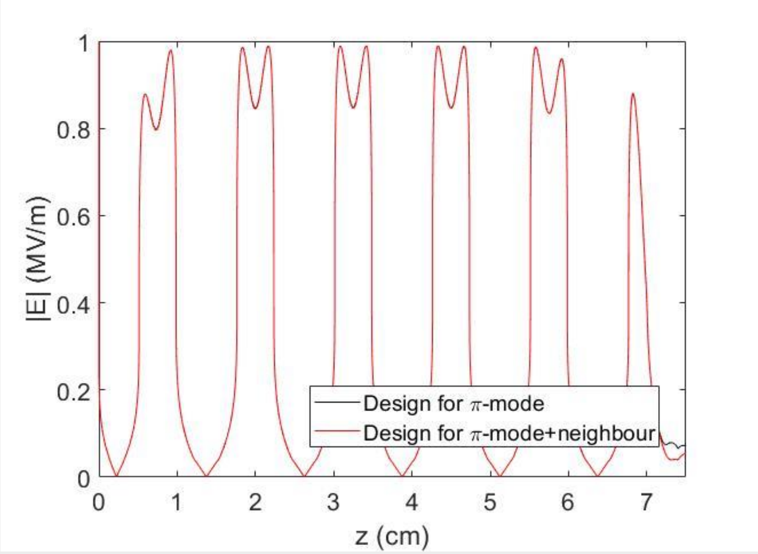

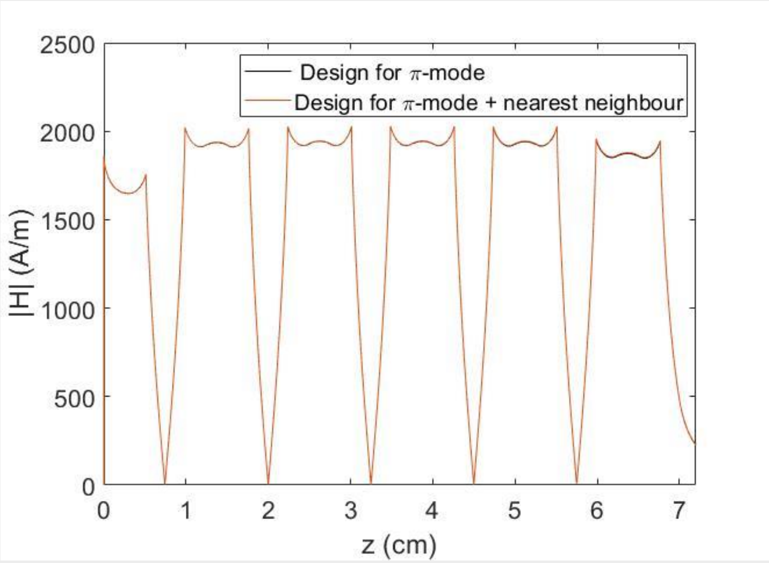

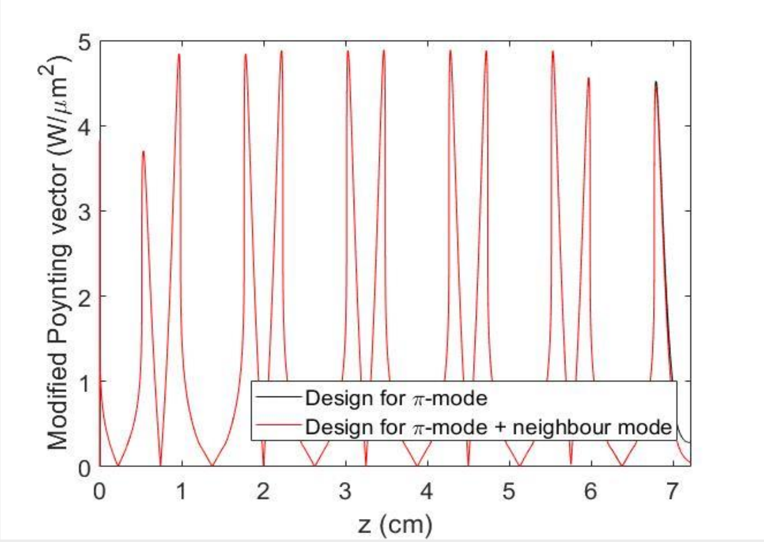

- It is observed that the RF electromagnetic pattern is the same for both RF gun designs

- Consequently, the results from the previous design involving the RF electromagnetic fields at surfaces (RF pulse heating, RF breakdown, multipactor) will still be valid for the new gun design

Funded by the
European Union

Summary

- In this slide is summarized the performance of the 5.6 cell X-band RF gun prototype

Parameter	
E_z flatness at peaks	>99 %
Resonant frequency, f_π	$11.9940380\ GHz$
Mode separation, Δf	27.1 MHz
Coupling factor, β	1.027
Filling time, t_F	112.5 ns
$max(E_{surf})$ for 1 MV/m at cathode	0.988 MV/m
BDR (for 400 ns pulse length)	$5.59 \times 10^{-6}\ bpp/m$
RF pulse heating (for 400 ns pulse length), max(ΔT)	31°C
Multipactor power zones	0.035-0.560 MW, 1.20-3.10 MW

Funded by the
European Union

Compact

Future work

➢ We will perform beam dynamics simulations with the *General Particle Tracer*[1] (GPT) software in order to study the beam performance in the 5.6 cell RF gun photoinjector

➢ It will be designed the solenoid for both emittance compensation and multipactor mitigation purposes

➢ A 4.6 cell RF gun photoinjector option will be designed, and its beam performance will be compared with the case of the 5.6 cell RF gun

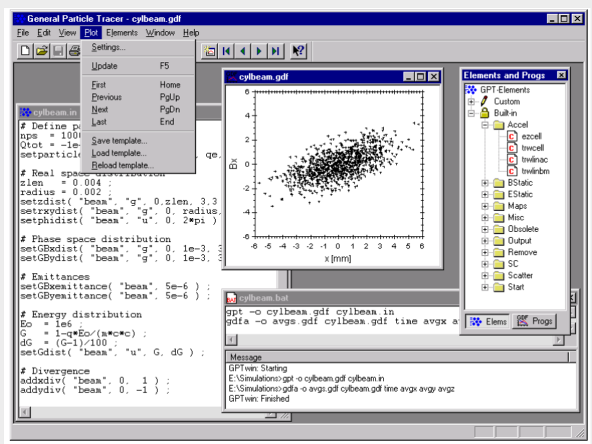

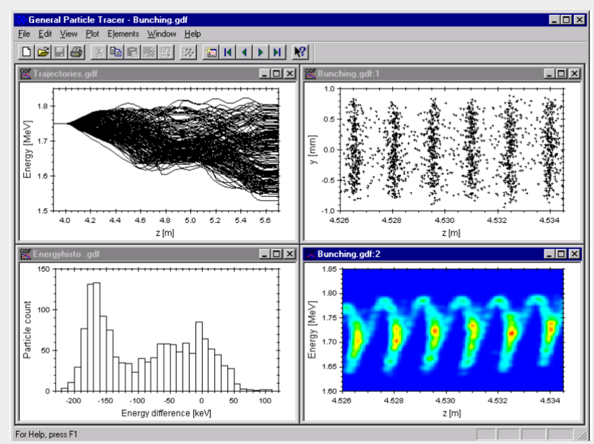

[1] http://www.pulsar.nl/gpt/

Some GPT screenshots

Funded by the European Union

Compact

Thank you!

CompactLight@elettra.eu

www.CompactLight.eu

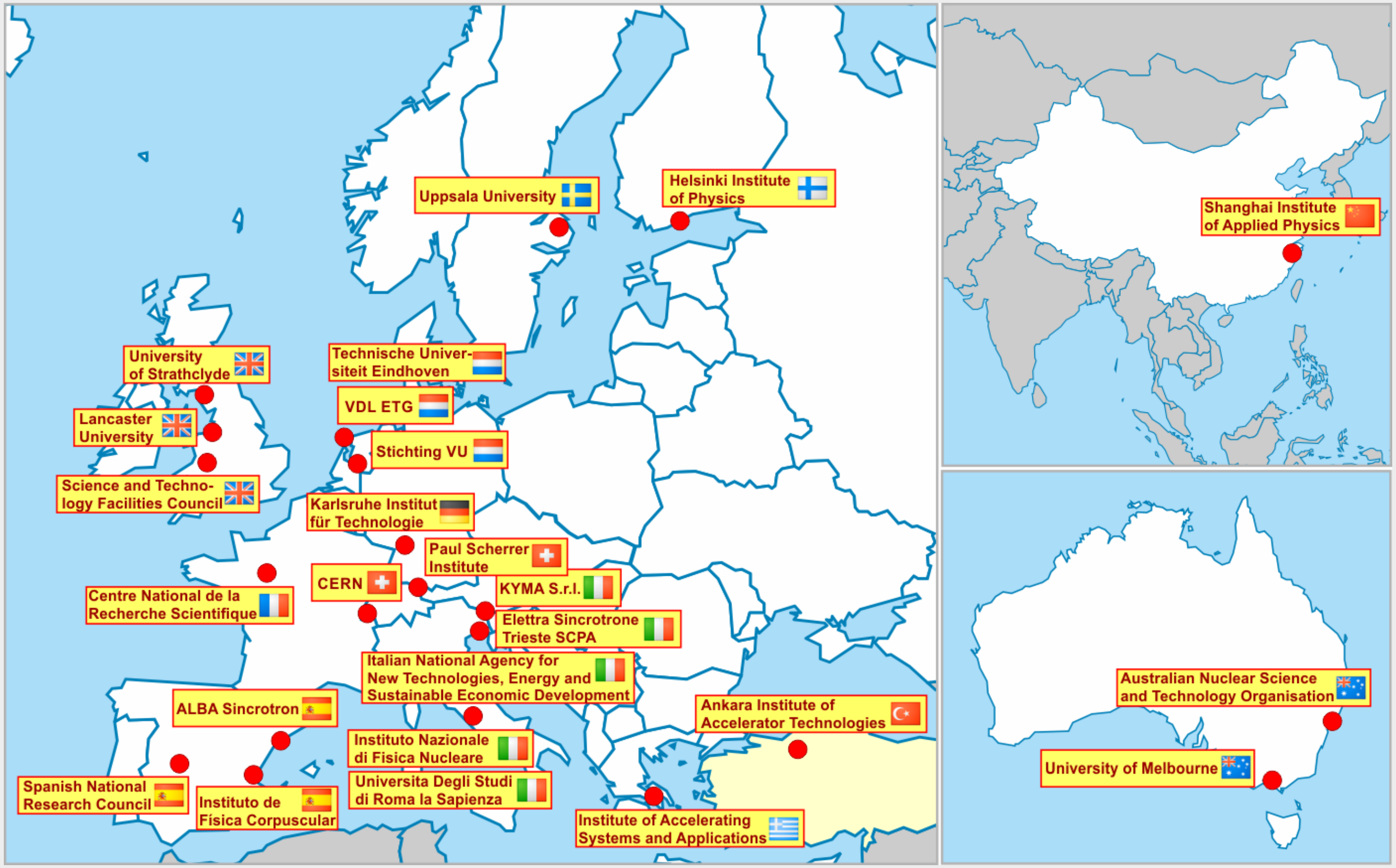

CompactLight is funded by the European Union's Horizon2020 research and innovation programme under Grant Agreement No. 777431.

Convergence analysis

- The convergence of the solution is checked by essaying different mesh size increments

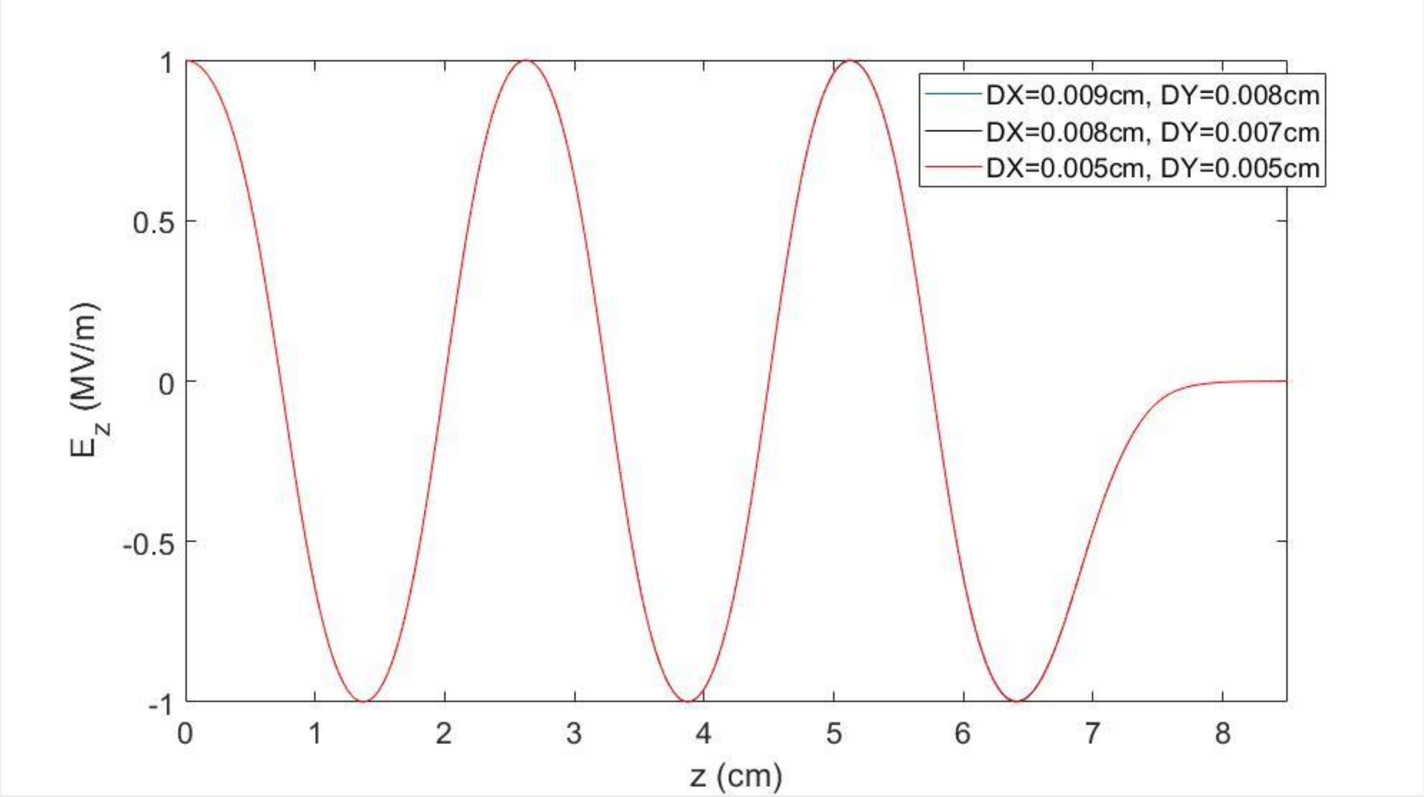

These are the mesh values employed in the design process

DX(cm), DY(cm)	f (GHz)	β	max(E_{sup}) (MV/m)
0.009, 0.008	11.99415	1.004	0.988
0.008, 0.007	11.99396	1.005	0.988
0.005, 0.005	11.99369	1.007	0.985

DX, DY are the mesh increments along the z and r directions, respectively

Study of the effect of neighbour cavity modes

- Despite the RF gun has been designed for operation with the π-mode, other neighbour modes present in the cavity might be excited during the transient regime

- To calculate the excitation of these neighbor modes, it is useful to use a equivalent circuital model to describe the mode excitation in the system composed by the RF generator, the coupler and the RF gun cavity[1,2]

$$\frac{\omega_m}{Q_0}\sqrt{\frac{\beta R}{Z_0}}V_{rf}(t) = \frac{dV_{cav}}{dt} + \frac{\omega_m}{Q_L}V_{cav} + \omega_m^2\int V_{cav}dt$$

$$\mathcal{L}\{V_{cav}(t)\} = \frac{\omega_m}{Q_0}\sqrt{\frac{\beta R}{Z_0}}\frac{s}{\left(s+\frac{\omega_m}{2Q_L}\right)^2 + \omega_m^2\left(1-\frac{1}{4Q_L^2}\right)}\mathcal{L}\{V_{rf}(t)\}$$

$$V_{rf}(t) = V_{rf,0}\sin(\omega t)H(t) \longrightarrow \mathcal{L}\{V_{rf}(t)\} = V_{rf,0}\frac{\omega}{s^2+\omega^2}$$

$$\mathcal{L}\{V_{cav}(t)\} = V_{rf,0}\frac{\omega\omega_m}{Q_0}\sqrt{\frac{\beta R}{Z_0}}\frac{s}{(s^2+\omega^2)\left[\left(s+\frac{\omega_m}{2Q_L}\right)^2 + \omega_m^2\left(1-\frac{1}{4Q_L^2}\right)\right]}\mathcal{L}\{V_{rf}(t)\}$$

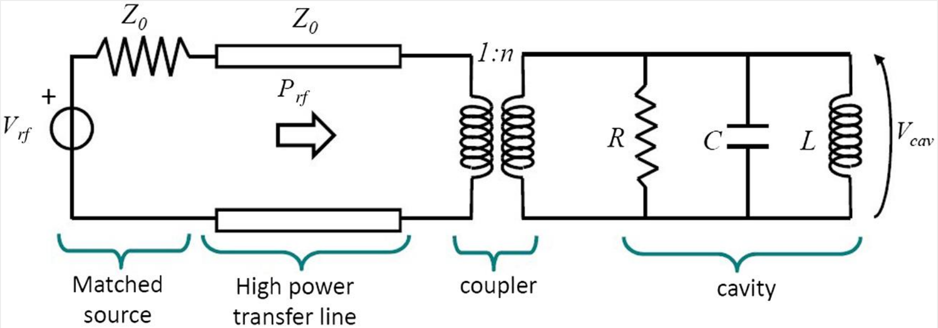

Equivalent circuit describing the RF generator, coupler and gun cavity (extracted from ref. 1)

β is the coupling factor
ω is the RF generator angular frequency
ω_m is the cavity mode angular frequency
R is the circuit resistance
Q_L is the loaded cavity quality factor
Q_0 is the unloaded cavity quality factor
Z_0 is the high power transfer line impedance
V_{rf} is the RF generator voltage
V_{cav} is the RF voltage in the gun cavity
$\mathcal{L}$ is the Laplace transform operator

[1] D. Alesini et al., "Design, realization, and high power test of high gradient, high repetition rate brazing-free S-band photogun", Physical Review Accelerators and Beams. 21, 112001 (2018)
[2] Thomas P. Wangler , "RF Linear Accelerators", Second Edition, 2008 WILEY-VCH Verlag GmbH & Co. KGaA

Study of the effect of neighbour cavity modes

- Finally the RF voltage for the m-mode at the gun cavity is

ω is the RF generator angular frequency
ω_m is the cavity mode angular frequency

$$V_{cav}(t) = V_{cav,0}\left[\sin(\omega t+\varphi_1) - \frac{e^{-\frac{\omega_m}{2Q_L}t}}{\sqrt{1-\frac{1}{4Q_L^2}}}\sin\left(\omega_m\sqrt{1-\frac{1}{4Q_L^2}}\,t+\varphi_2\right)\right]$$

$$V_{cav,0} = V_{rf,0}\frac{\omega_m\omega}{Q_0}\sqrt{\frac{\beta R}{Z_0}}\frac{1}{\sqrt{\left(\frac{\omega\omega_m}{Q_L}\right)^2+(\omega_m^2-\omega^2)^2}}$$

$$\tan\varphi_1 = Q_L\frac{\omega_m^2-\omega^2}{\omega\omega_m} \qquad \tan\varphi_2 = \sqrt{4Q_L^2-1}\,\frac{\omega_m^2-\omega^2}{\omega_m^2+\omega^2}$$

For $t \gg \frac{\omega_m}{2Q_L}$ → $V_{cav}(t) \simeq V_{cav,0}[\sin(\omega t+\varphi_1)]$

- The RF cavity voltage can be related to the RF electric field amplitude at cathode

$$E_z(r=0,z) = E_z(z) = E_{0,cath}\,g(z) \quad , \quad g(z)\mid g(0)=1$$

$$V_{cav,0} \equiv \int_0^L E_z(z)dz = E_{0,cath}\int_0^L g(z)dz \rightarrow E_{0,cath} = \frac{V_{cav,0}}{\int_0^L g(z)dz}$$

$$R = \frac{r_s}{2} \equiv \frac{1}{2}\frac{V_{cav,0,Pdiss}^2}{P_{diss}} = \frac{E_{0,cath,Pdiss}^2\left(\int_0^L g(z)dz\right)^2}{2P_{diss}} \rightarrow \int_0^L g(z)dz = \frac{\sqrt{2P_{diss}R}}{E_{0,cath,Pdiss}} \rightarrow E_{0,cath} = \frac{V_{cav,0}E_{0,cath,Pdiss}}{\sqrt{2P_{diss}R}}$$

$$\alpha_m = \frac{E_{0,cath,Pdiss}}{\sqrt{2P_{diss}}}$$

$$E_{0,cath} = V_{rf,0}\frac{\omega_m\omega}{Q_0}\sqrt{\frac{\beta}{Z_0}}\frac{\alpha_m}{\sqrt{\left(\frac{\omega\omega_m}{Q_L}\right)^2+(\omega_m^2-\omega^2)^2}}$$

$$E_{0,cath}(t) = E_{0,cath}\left[\sin(\omega t+\varphi_1) - \frac{e^{-\frac{\omega_m}{2Q_L}t}}{\sqrt{1-\frac{1}{4Q_L^2}}}\sin\left(\omega_m\sqrt{1-\frac{1}{4Q_L^2}}\,t+\varphi_2\right)\right]$$

Study of the effect of neighbour cavity modes

➢ Using the previous expressions, the time variation of the RF electric field at cathode can be depicted as it is shown next:

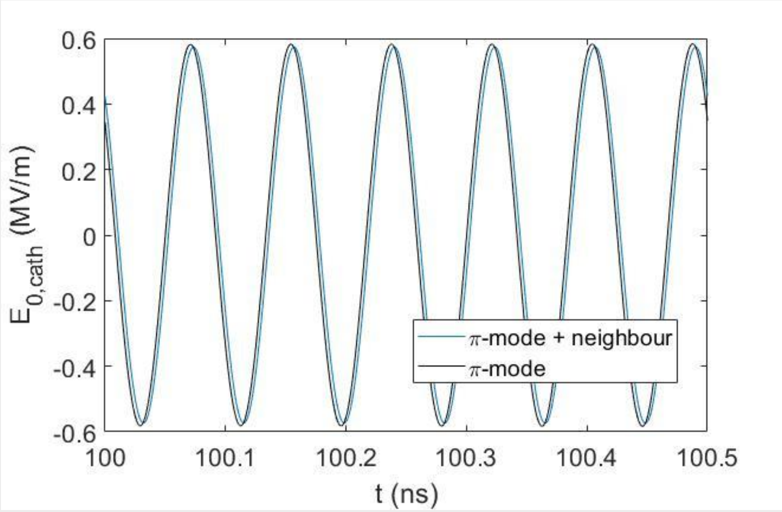

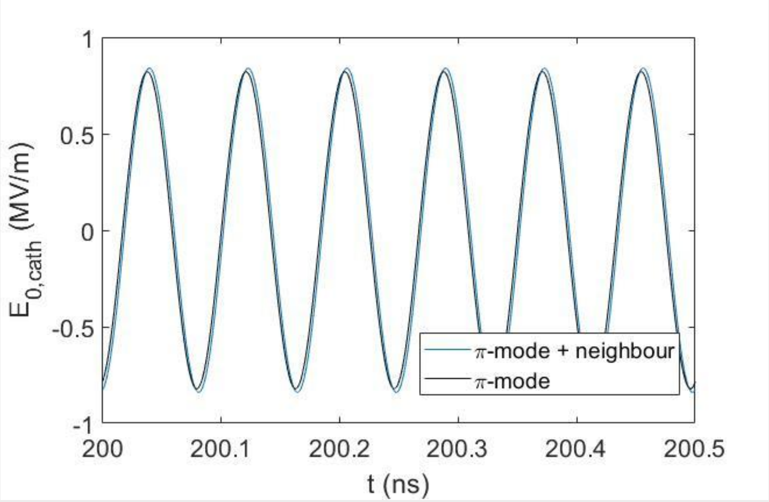

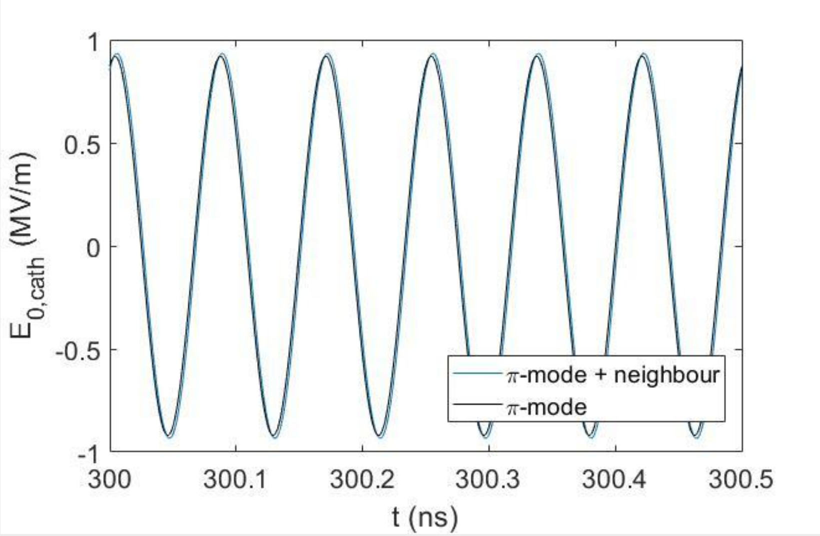

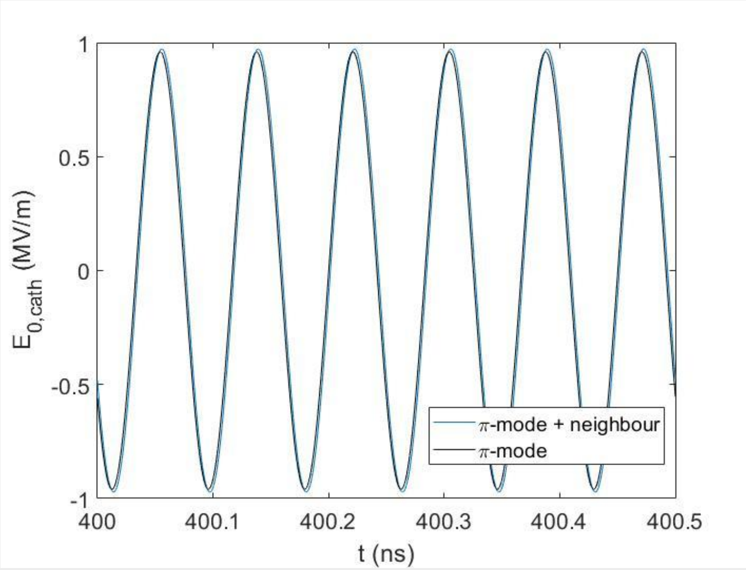

Study of the effect of neighbour cavity modes

- To validate the previous results obtained from SUPERFISH plus the circuital model treatment, a comparison with the results obtained from HFSS simulations is presented:

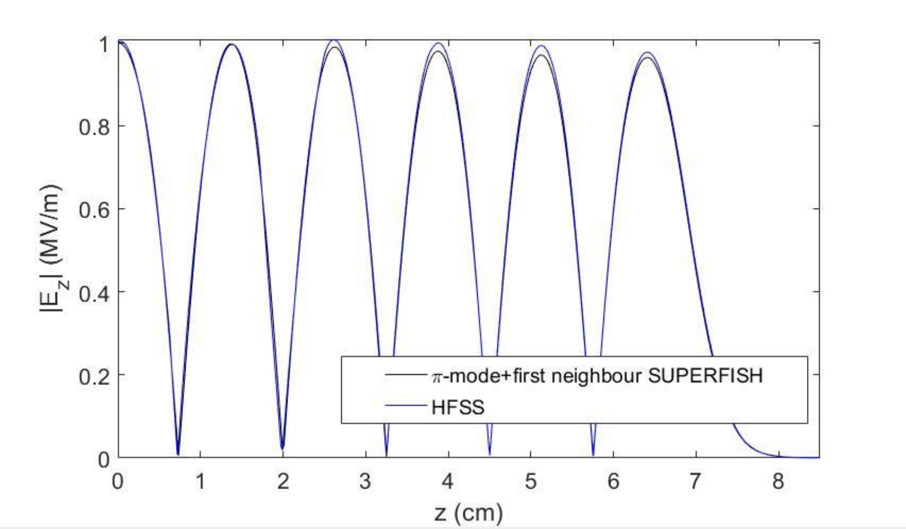

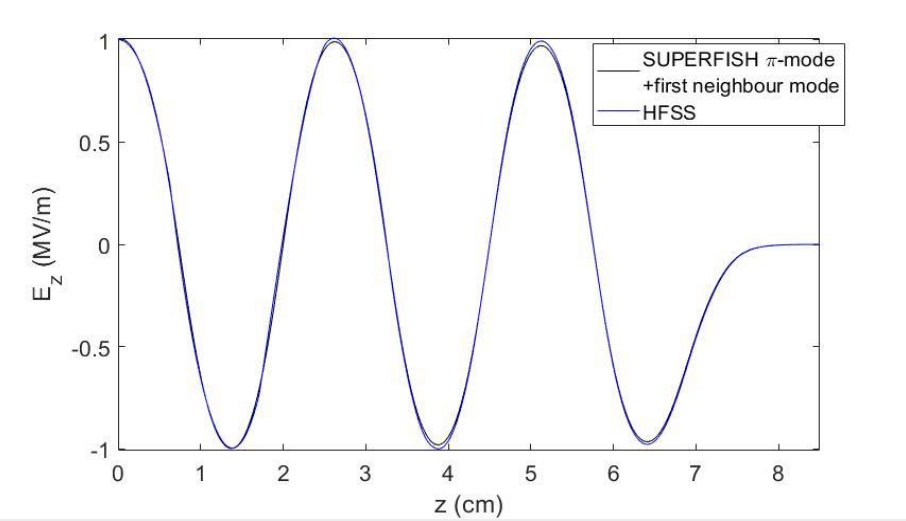

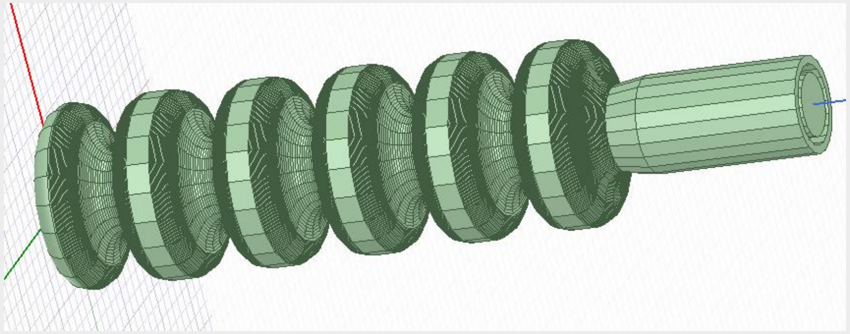

3D view of the RF gun with HFSS

- It is evidenced the good agreement between the results obtained from HFSS and with SUPERFISH using the circuital model treatment

RF power system